PIGMENT CELL & MELANOMA Research

Anti-melanogenic effect of exosomes derived from human dermal fibroblasts (BJ-5ta-Ex) in C57BL/6 mice and B16F10 melanoma cells

Jung Min Lee | Jung Ok Lee | Yujin Kim | You Na Jang |
A. Yeon Park | Su-Young Kim | Hye Sung Han |
Beom Joon Kim | Kwang Ho Yoo

INTERNATIONAL FEDERATION OF PIGMENT CELL SOCIETIES · SOCIETY FOR MELANOMA RESEARCH

The official journal of

PIGMENT & MELANOMA

Research

Volume 26 · Number 1 · January 2013

WILEY-BLACKWELL
www.pigment.org

Vitamin D in melanoma
KIT variants and melanoma risk
The biology of rapid colour change

If you wish to order reprints of this article,
please see the guidelines **here**

Supporting Information for this article is freely available **here**

EMAIL ALERTS
Receive free email alerts and stay up-to-date on what is published
in Pigment Cell & Melanoma Research – **click here**

Submit your next paper to PCMR online at http://mc.manuscriptcentral.com/pcmr

Subscribe to PCMR and stay up-to-date with the only journal committed to publishing
basic research in melanoma and pigment cell biology

As a member of the IFPCS or the SMR you automatically get online access to PCMR. Sign up as
a member today at **www.ifpcs.org** or at **www.societymelanomaresarch.org**

To take out a personal subscription, please click here
More information about Pigment Cell & Melanoma Research at **www.pigment.org**
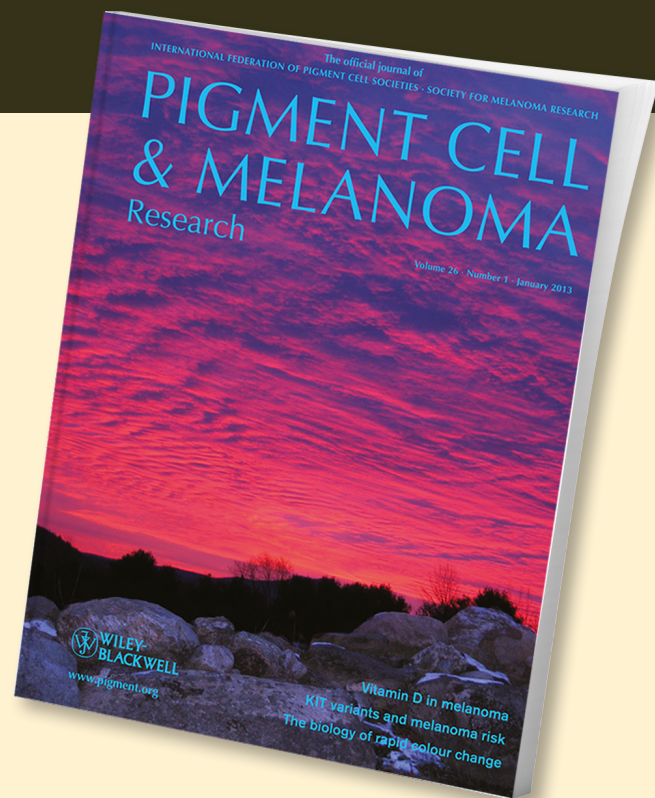
ORIGINAL ARTICLE

WILEY

Anti-melanogenic effect of exosomes derived from human dermal fibroblasts (BJ-5ta-Ex) in C57BL/6 mice and B16F10 melanoma cells

Jung Min Lee[1] | Jung Ok Lee[1] | Yujin Kim[1,2] | You Na Jang[1] | A. Yeon Park[1,2] | Su-Young Kim[1,2] | Hye Sung Han[3] | Beom Joon Kim[1,2] | Kwang Ho Yoo[3]

[1]Department of Dermatology, College of Medicine, Chung-Ang University, Seoul, South Korea

[2]Department of Medicine, Graduate School, Chung-Ang University, Seoul, South Korea

[3]Department of Dermatology, Chung-Ang University Gwang-Myeong Hospital, Chung-Ang University College of Medicine, Gwangmyeong, South Korea

Correspondence
Kwang Ho Yoo, Department of Dermatology, Chung-Ang University Gwang-Myeong Hospital, Chung-Ang University College of Medicine, 110 Deokan-ro, Gwangmyeong-si, Gyeonggi-do 14353, South Korea.
Email: psyfan9077@naver.com

Beom Joon Kim, Department of Dermatology, College of Medicine, Chung-Ang University Hospital, 102 Heukseok-ro, Dongjak-gu, Seoul 06973, South Korea.
Email: beomjoon74@gmail.com

Abstract

Exosomes are involved in intercellular communication by transferring cargo between cells and altering the specific functions of the target cells. Recent studies have demonstrated the therapeutic effects of exosomes in several skin diseases. However, understanding of the effects of exosomes on anti-pigmentation is limited. Therefore, we investigated whether BJ-5ta exosomes (BJ-5ta-Ex) derived from human foreskin fibroblasts regulate melanogenesis and delineated the underlying mechanism. Interestingly, treatment with BJ-5ta-Ex induced decreased melanin content, tyrosinase (TYR) activity, and expression of melanogenesis-related genes, including microphthalmia-related transcription factor (MITF), TYR, tyrosinase-related protein-1 (TRP1), and tyrosinase-related protein-2 (TRP2). In addition, BJ-5ta-Ex downregulated the cAMP/PKA and GSK-3β/β-catenin signaling pathways and upregulated the MAPK/ERK signaling pathway. Notably, treatment with BJ-5ta-Ex inhibited α-melanocyte-stimulating hormone-induced melanosome transport and decreased the expression of key proteins involved in melanosome transport, namely, rab27a and melanophilin (MLPH). To further confirm the depigmenting effects of BJ-5ta-Ex, we conducted experiments using a three-dimensional reconstituted human full skin model and ultraviolet B (UVB)-irradiated mouse model. Treatment with BJ-5ta-Ex improved tissue brightness and reduced the distribution of melanosomes. In UVB-irradiated mouse ears, BJ-5ta-Ex reduced the number of active melanocytes and melanin granules. These results demonstrate that BJ-5ta-Ex can be useful for the clinical treatment of hyperpigmentation disorders.

KEYWORDS
ERK signaling, exosomes, melanogenesis, melanosome transport, MITF

Jung Min Lee and Jung Ok Lee contributed equally to this work.

1 | INTRODUCTION

Melanin is responsible for the pigmentation of the skin and hair (Clarys et al., 2000). This pigment also protects keratinocytes within skin from ultraviolet (UV)-induced DNA damage (Shoag et al., 2013). However, excessive production and irregular accumulation of melanin can lead to several skin abnormalities, such as melasma, freckles, and age spots (Speeckaert et al., 2014). Thus, there is a significant interest in developing depigmentation agents to prevent or treat skin hyperpigmentation for medical or cosmetic reasons.

Melanogenesis occurs through complex enzymatic and biochemical catalytic reactions. The three major regulators of melanin synthesis are tyrosinase (TYR), tyrosinase-related protein 1 (TRP1), and tyrosinase-related protein 2 (TRP2) (Hearing, 2011). Microphthalmia-associated transcription factor (MITF) is a master transcription factor that activates the transcription of pigmentation genes, including TYR, TRP1, and TRP2. MITF is also required for melanocyte proliferation and differentiation (Hsiao & Fisher, 2014).

Pigmentation is regulated by complex signaling transduction cascades in melanocytes. The cyclic adenosine monophosphate (cAMP)-response element binding protein (CREB) signaling pathway is mainly activated by alpha-melanocyte-stimulating hormone (α-MSH) from keratinocytes. The increase in intracellular cAMP promotes the phosphorylation of CREB, a co-factor involved in cAMP-dependent MITF expression, which in turn binds to the *MITF* gene promoter and stimulates the expression levels of MITF. The induced MITF stimulates downstream target melanogenic genes such as TYR, TRP1, and TRP2, resulting in the production of melanin pigment (Busca & Ballotti, 2000; Niu & Aisa, 2017).

There are three key proteins involved in melanosome transportation: rab27a, melanophilin (MLPH), and myosin 5a. These proteins form a tripartite complex and connect the melanosome to the actin cytoskeleton (Hume et al., 2006). Rab27a is a small GTPase protein present on the membrane of mature melanosomes and plays a role in intracellular vesicular transport and organelle dynamics (Fukuda, 2021; Hume et al., 2007). MLPH serves as the effector of rab27a and interacts directly with the GTP-bound form of rab27a and Myosin-Va. Myosin-Va is responsible for the trafficking of melanosomes in melanocytes. In brief, Rab27a captures the melanosome, myosin-Va binds to actin filaments, and these two proteins are linked by MLPH (Wu et al., 2006).

Regulation of melanogenesis could be an important strategy for treating abnormal skin pigmentation. For instance, skin whitening agents, such as KA, arbutin, and hydroquinone, have been used to prevent or treat skin hyperpigmentation (Nakagawa et al., 1995). These agents inhibit melanogenesis by controlling TYR activity (Desmedt et al., 2016). However, hydroquinone has been banned or restricted as a cosmetic agent in many countries due to its toxic effects on mammalian cells, including contact dermatitis, irritation, burning, and hypopigmentation (Chang et al., 2017). In addition, KA is associated with carcinogenicity and is unstable (Zilles et al., 2022).

Significance

Skin whitening agents, such as kojic acid (KA) and hydroquinone, have been developed, but they are associated with toxicity and are unstable. In contrast, exosomes have notable stability and low associated tumorigenesis. There is limited research on the whitening effects of fibroblast-derived exosomes. Therefore, we examined the effect of BJ-5ta-Ex on melanogenesis. We found that BJ-5ta-Ex prevent melanogenesis by decreasing melanin content, TYR activity, and the expression of melanogenesis-related genes such as TYR, TRP1, and TRP2. In addition, BJ-5ta-Ex increased brightness and reduced the distribution of pigmentation in a 3D human full skin model and a UVB-irradiated mouse model. These findings demonstrated that BJ-5ta-Ex have potential preventive or therapeutic effects for improving hyperpigmentation disorders.

Therefore, there is an unmet need to develop a safe and effective treatment regimen that can attenuate hyperpigmentation.

Exosomes are extracellular vesicles derived from cells, with a diameter of 40–160 nm (Gaur et al., 2017). They have the capacity to carry various biomolecules, including proteins, carbohydrates, lipids, and nucleic acids, enabling communication with adjacent or distant cells. Exosomes have recently garnered significant interest because of their high biocompatibility and potent immunomodulatory effects (Zhang et al., 2019). In particular, exosomes have been explored as a cell-free therapeutic approach for various skin diseases, including wound healing (exosomes from keratinocyte), psoriasis (exosomes from keratinocyte), and atopic dermatitis (AD) (exosomes from keratinocyte) (Cho et al., 2018; Jiang et al., 2019; Li et al., 2019).

However, the effect of fibroblast-derived exosomes on melanogenesis has yet to be evaluated. Therefore, in this study, we prepared foreskin dermal fibroblast-derived exosomes (BJ-5ta-Ex) and examined their effects on anti-pigmentation using in vitro and in vivo models.

2 | MATERIALS AND METHODS

2.1 | Culture of B16F10 cells and reagents

B16F10 mouse melanoma cells were purchased from the American Type Culture Collection (ATCC, VA, USA). B16F10 cells were cultured in Dulbecco's modified Eagle's medium (DMEM) containing 10% fetal bovine serum (FBS) and 1% penicillin/streptomycin at 37°C with 5% CO_2. α-MSH, KA, arbutin, and PD98059 were purchased from Sigma-Aldrich (MO, USA). BIO was purchased from Selleckchem (Texas, USA).

2.2 | Isolation and characterization of exosomes

Human immortalized foreskin fibroblasts (BJ-5ta cells) were purchased from Gibco (MD, USA). BJ-5ta-Ex were isolated from the cell supernatants. BJ-5ta cells were incubated in serum-free DMEM until they reached 70%–80% confluence. Then, the conditioned medium was collected and centrifuged at $300 \times g$ for 10 min followed by centrifugation at $2000 \times g$ for 20 min. The cells and cellular debris were removed by filtration, and the supernatant was collected and concentrated using a sterile-membrane T-series cassette (Pall Life Sciences, NY, USA) with tangential flow filtration. The mixture was centrifuged at $100,000 \times g$ for 3 h. The morphological feature of BJ-5ta-Ex was determined using field-emission scanning electron microscopy (FE-SEM) (Carl Zeiss Meditec AG, Jena, Germany). The size distribution was determined using nanoparticle tracking analysis (NTA) on ZetaView (Particle Metrix, Diessen, Germany). Fibroblast-derived exosomal markers, including ALIX, CD63, and β-actin, were quantified using western blot analysis with calnexin as a negative control.

2.3 | Assessment of cell viability

B16F10 cells were seeded in 96-well plates at a density of 3×10^3 cells/well. The cells were exposed to BJ-5ta-Ex at concentrations ranging between 10^3 and 10^9 particles/mL for 24 h. The cells were incubated in a medium containing WST-8 solution for 1 h at 37°C with 5% CO_2. The absorbance was measured at 450 nm using a SpectraMax i3x spectrophotometer (Molecular Devices, CA, USA).

2.4 | Measurement of melanin content

B16F10 cells were seeded in a 24-well plate (10^4 cells/dish) and incubated overnight at 37°C. Cells were pretreated with BJ-5ta-Ex for 24 h and, after 48 h, they were exposed to 100 nM α-MSH. Cellular melanin was dissolved in 200 μL of 1 N NaOH–10% DMSO for 1 h at 60°C, and the solubilized melanin content was photographed with a digital camera and measured at 405 nm using a SpectraMax i3x spectrophotometer (Molecular Devices).

2.5 | Intracellular tyrosinase activity

The cells were lysed in 150 μL of lysis buffer. The lysates were centrifuged at 13,000 rpm for 20 min at 4°C, the supernatant was collected, and the protein concentration was measured. The samples were (100 μL) transferred to a 96-well plate, and the enzymatic assay was initiated by adding 100 μL of L-DOPA solution (0.1% in PBS, pH 6.8) at 37°C. The absorbance was measured at 475 nm using a SpectraMax i3x spectrophotometer.

2.6 | In situ intracellular tyrosinase activity

B16F10 cells were pretreated with BJ-5ta-Ex for 24 h and then co-treated with α-MSH. The cells were fixed with 4% paraformaldehyde (PFA) for 30 min, followed by treatment with 0.1% triton X-100 for 2 min. L-DOPA (0.1%) was added to each well, and the plates were incubated for 3 h. The cells were observed under a microscope.

2.7 | Reverse transcription-quantitative PCR (RT-qPCR)

Total RNA was extracted using TRIzol Reagent (Invitrogen, CA, USA). Single-strand cDNA synthesis was performed using Prime-Script TM RT Master Mix (Takara, Tokyo, Japan). The resulting cDNA was subjected to RT-qPCR on a CFX96 thermocycler (Bio-Rad, CA, USA) using RT-qPCR PreMIX SYBR Green (Enzynomics, Seoul, Korea). Gene expression levels were calculated as a cycle threshold (Ct) value using the $2^{-\Delta\Delta CT}$ quantification method and normalized to that of glyceraldehyde-3-phosphate dehydrogenase (GAPDH). The primers used for qPCR are listed in Table 1.

2.8 | Western blot analysis

Equal amounts of protein were resolved on a 10% sodium dodecyl-sulfate polyacrylamide (SDS-PAGE) gel through electrophoresis and transferred to a nitrocellulose membrane (Cytiva, Amersham, USA). Membranes were blocked in 5% skim milk in Tris-buffered saline (TBS) containing 0.1% Tween-20 (TBS-T) and probed overnight at 4°C with primary antibodies. The antibodies used are listed in Table 2. The membranes were washed

TABLE 1 Primer sequences used for quantification of gene expression.

Gene	Primer sequence (5′→3′)
Mouse MITF	
F	AGTACAGGAGCTGGAGATG
R	GTGAGATCCAGAGTTGTCGT
Mouse tyrosinase	
F	GAGAAGCGAGTCTTGATTAG
R	TGGTGCTTCATGCGCAAAATC
Mouse TRP1	
F	AGCCCCAACTCTGTCTTTTC
R	GGTCTCCCTACATTTCCAGC
Mouse TRP2	
F	CAGTTTCCCCGAGTCTGCAT
R	GTCTAAGGCGCCCAAGAACT
Mouse GAPDH	
F	AGGTCGGTGTGAACGGATTTG
R	TGTAGACCATGTAGTTGAGGTCA

TABLE 2 Antibodies used for western blot analysis.

Antibodies	Product code	Company
Anti-MITF	MAB3747-I	Sigma-Aldrich (MO, USA)
Anti-Calnexin	ab22595	Abcam (Cambridge, UK)
Anti-ALIX	ab275377	Abcam (Cambridge, UK)
Anti-CD63	ab134045	Abcam (Cambridge, UK)
Anti-tyrosinase	ab180753	Abcam (Cambridge, UK)
Anti-p-MITF	ab59201	Abcam (Cambridge, UK)
Anti-TRP-1	sc-58437	Santa Cruz Biotechnology (CA, USA)
Anti-TRP-2	sc-25544	Santa Cruz Biotechnology (CA, USA)
Anti-Rab27a	sc-22756	Santa Cruz Biotechnology (CA, USA)
Anti-β-actin	sc-47778	Santa Cruz Biotechnology (CA, USA)
Anti-p-CREB	#9198	Cell Signaling Technology Inc. (Beverly, MA)
Anti-CREB	#9197	Cell Signaling Technology Inc. (Beverly, MA)
Anti-p-ERK	#9101	Cell Signaling Technology Inc. (Beverly, MA)
Anti-ERK	#9102	Cell Signaling Technology Inc. (Beverly, MA)
Anti-p-AKT	#4060	Cell Signaling Technology Inc. (Beverly, MA)
Anti-AKT	#4691	Cell Signaling Technology Inc. (Beverly, MA)
Anti-p-β-catenin	#4176	Cell Signaling Technology Inc. (Beverly, MA)
Anti-β-catenin	#8480	Cell Signaling Technology Inc. (Beverly, MA)
Anti-Myosin-Va	#3402	Cell Signaling Technology Inc. (Beverly, MA)
Anti-MLPH	10338-1-AP	ProteinTech Group (IL, USA)

and incubated with horseradish peroxidase (HRP)-conjugated anti-mouse (Vector Laboratories Inc., CA, USA) or anti-rabbit (Vector Laboratories Inc.) secondary antibodies. Immunodetection was performed using an Amersham ECL kit (GE Healthcare, IL, USA) according to the manufacturer's protocol. The protein bands were visualized using a ChemiDoc™ MP Imaging System (Bio-Rad Laboratories, Inc., Hercules, CA, USA) and analyzed using the NIH Image J software (Bethesda, MD, USA).

2.9 | Immunocytochemistry (ICC)

The cells were fixed with 4% PFA for 30 min, washed with PBS, blocked with 3% BSA and 0.2% Triton X-100 in PBS for 1 h at room temperature (RT), and incubated overnight at 4°C with primary antibodies. After washing with PBS, the cells were incubated with anti-rabbit, mouse IgG-FITC secondary antibodies for 1 h at RT in dark. The cell nuclei were counterstained with DAPI (Immuno Bioscience Corp., Washington, USA), and F-actin was stained with phalloidin (Thermo Fisher Scientific, MA, USA). The cells were observed by fluorescence microscopy (DMi8, Leica, Wetzlar, Germany).

2.10 | Measurement of cAMP levels

The cAMP levels were determined using a cAMP immunoassay kit (Cayman Chemical Company, Ann Arbor, MI, USA). B16F10 cells were lysed in 0.1 M HCl to inhibit phosphodiesterase activity and incubated at RT for 20 min. The lysates were centrifuged at $1000 \times g$ for 10 min. Supernatants were collected in a tube. The lysates were transferred to a 96-well plate coated with rabbit IgG polyclonal antibody and incubated concomitantly with a constant concentration of cAMP-acetylcholinesterase (Ache) conjugate (Tracer) as a competitor of cAMP in the well. After incubation at 4°C for 18 h, the wells were washed to remove the unbound cAMP, and Ellman's reagent was added to determine the activity of cAMP. The optical density was detected at 420 nm, which is proportional to the amount of the cAMP Tracer but inversely proportional to the concentration of cAMP in the wells.

2.11 | Mouse experiments

C57BL/6 mice (9-week-old males) were obtained from Saeron Bio Inc. (Gyeonggi-do, Korea) and acclimated for 7 days at a temperature of $23 \pm 2°C$, with a humidity level of $55\% \pm 10\%$ and a 12-h light/12-h dark cycle. All animal experiments were conducted according to the Principles of Laboratory Animal Care established by the National Institutes of Health (NIH) and were approved by the Chung-Ang University Institutional Animal Care and Use Committee (IACUC no. 202301020004). Prior to evaluation, the animals were anesthetized with Zoletil (40 mg/kg) and Rompun (5 mg/kg). The animals were randomly divided into five groups: normal control ($N=6$), UVB ($N=6$), UVB+BJ-5ta-Ex at a dose of 10^7 particles/kg ($N=6$), UVB+BJ-5ta-Ex at a dose of 10^8 particles/kg ($N=6$), and UVB+arbutin (30 mg/kg) ($N=6$). Pigmentation was induced through UVB irradiation using a BIO-SPECTRA (Vilber Lourmat, Collégien, France) three times a week for 2 weeks. The initial dose of UVB irradiation was 150 mJ/cm^2 for a week, and the dose was increased to 200 mJ/cm^2 the following week.

The ears were treated with BJ-5ta-Ex at doses of 10^7 particles/kg and 10^8 particles/kg daily for 3 weeks.

2.12 | Reconstructed human skin model

The reconstructed human skin model Neoderm-M was purchased from Tego Science (Seoul, Korea). Neoderm-M was removed from medium-containing agar and transferred onto 12-well plates for equilibration at 37°C (5% CO_2) for 1 day. Under treatment with BJ-5ta-Ex or arbutin, Neoderm-M was irradiated with UVB (50 mJ/cm^2) every other day for a total of four exposures, and the tissue samples were kept in an incubator at 37°C (5% CO_2). To compare the anti-melanogenesis effect, the reconstructed human skin was photographed with a digital camera on day 8.

2.13 | Histological observation and immunohistochemistry (IHC)

The reconstructed human skin and mouse ear samples were fixed in 10% formalin for 24 h, dehydrated in ethanol, embedded in paraffin, sectioned, and stained with hematoxylin and eosin (H&E) and Fontana–Masson (F–M). IHC was performed on the sections. Tissues were then subjected to antigen retrieval with Tris-EDTA at 4°C for 15 min and treated with BLOCKALLTM Blocking Solution for 10 min. The slides were incubated with 2.5% normal horse serum and stained with primary antibodies overnight at 4°C. The slides were then incubated with HRP using the ImmPRESS® Excel Amplified Polymer Staining Kit (Vector Laboratories Inc.), and the staining was developed using the 3,3′-diaminobenzidine (DAB) peroxidase substrate kit (Vector Laboratories Inc.). To identify nuclei, slides were counterstained with hematoxylin.
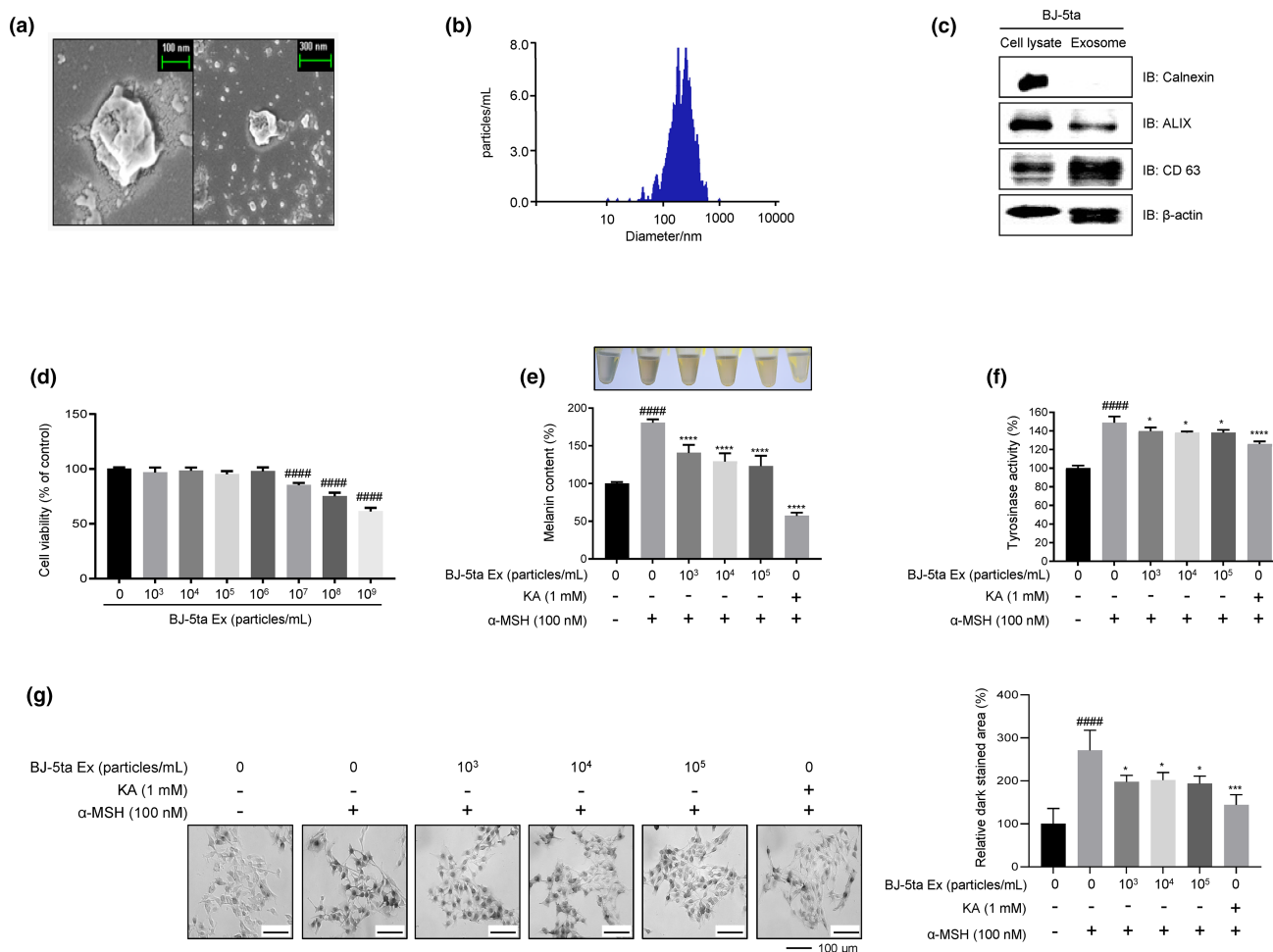

FIGURE 1 Characterization of BJ-5ta-Ex and the effect of BJ-5ta-Ex on cytotoxicity, melanin content, and TYR activity in B16F10 cells. (a) The morphology of BJ-5ta-Ex was observed using FE-SEM (scale bars, 100, 300 μm). (b) The size distribution of BJ-5ta-Ex was assessed using NTA. (c) The expression of calnexin, ALIX, and CD63 in BJ-5ta-Ex was assessed by western blotting. (d) B16F10 cells were treated with BJ-5ta-Ex for 24 h; subsequently, a WST-8 cell viability assay was performed. (e) The melanin content in B16F10 cells exposed to α-MSH (100 nM) for 48 h and pretreated with BJ-5ta-Ex or KA (1 mM) was photographed with a digital camera and measured at 405 nm using a SpectraMax i3x spectrophotometer. (f) The intracellular tyrosinase activity was determined using lysates obtained from B16F10 cells treated with BJ-5ta-Ex or KA. (g) In situ intracellular tyrosinase activity observed by L-DOPA staining. Scale bar = 100 μm. The results are expressed as the mean ± standard deviation. ####$p < .0001$ compared with the control group (untreated group). *$p < .05$, **$p < .01$, ****$p < .0001$ compared with the α-MSH-treated group.

2.14 | Statistical analysis

The results are expressed as the mean±standard deviation (SD) of at least three independent experiments. The data were analyzed using one-way ANOVA followed by a Bonferroni post hoc test. All statistical analyses were performed using the GraphPad Prism 7.0 software (GraphPad Software Inc., CA, USA). Differences with p values lower than .05 were considered statistically significant and are indicated on graphs with the following symbols: $*p < .05$; $**p < .01$; $***p < .001$; and $****p < .0001$.

3 | RESULTS

3.1 | BJ-5ta-Ex inhibit α-MSH-induced melanogenesis in B16F10 cells

BJ-5ta-Ex exhibited a spherical morphology (Figure 1a). The diameters of most BJ-5ta-Ex ranged from 100 to 300nm (Figure 1b). Exosome markers including CD63 and ALIX (Hong et al., 2019) were detected in BJ-5ta-Ex, whereas the negative control calnexin was not detected (Figure 1c). These results indicate that highly pure BJ-5ta-Ex were successfully obtained. To examine the cytotoxicity of BJ-5ta-Ex on B16F10 cells, we performed a WST-8 assay. No cytotoxicity was observed at doses of up to 10^6 particles/mL (Figure 1d). However, cytotoxicity was detected starting at the dose of 10^7 particles/mL. As a melanin synthesis inducer, α-MSH was used, while KA, a tyrosinase inhibitor, served as a positive control. The melanin content of α-MSH-stimulated cells increased approximately 1.8-fold compared with vehicle-treated control cells. In contrast, BJ-5ta-Ex at doses of 10^3, 10^4, and 10^5 particles/mL significantly decreased melanin production by 40%, 51.6%, and 57.8%, respectively, compared with that in α-MSH-stimulated B16F10 cells. Moreover, 1mM KA also reduced melanin levels by 123.5% compared with α-MSH-stimulated cells (Figure 1e). To elucidate the tyrosinase inhibitory effect of BJ-5ta-Ex, we assessed the intracellular tyrosinase activity and in situ intracellular tyrosinase activity. As expected, an approximately 1.5-fold increase in cellular tyrosinase activity was observed in α-MSH-stimulated cells compared with unstimulated cells. The tyrosinase activity in cells treated with BJ-5ta-Ex at doses of 10^3, 10^4, and 10^5 particles/mL was reduced by 9.3%, 10.8%, and 10.9%, respectively, compared with that in α-MSH-stimulated cells. KA reduced tyrosinase activity by 23.1% (Figure 1f). We further confirmed the anti-melanogenic effect of BJ-5ta-Ex by L-3,4-dihydroxyphenylalanine (L-DOPA) staining, which detects in situ tyrosinase activity (Figure 1g). These results indicated that the inhibitory effect of BJ-5ta-Ex on melanogenesis was not due to direct inhibition of tyrosinase.

3.2 | BJ-5ta-Ex suppress the expression of melanogenesis-associated genes

Treatment with α-MSH increased the mRNA and protein levels of MITF, TYR, TRP1, and TRP2. Treatment with BJ-5ta-Ex prior to stimulation with α-MSH significantly decreased the expression levels of these proteins and mRNA, especially those of MITF, TRP1, and TRP2 (Figure 2a,b). MITF, which is only expressed in the nucleus, is a transcription factor that regulates melanogenesis by activating the transcription of TYR, TRP1, and TRP2 (Hsiao & Fisher, 2014). Exposure to BJ-5ta-Ex also reduced α-MSH-mediated MITF expression in the nucleus (Figure 2c). These results indicate that suppression of the expression of TYR, TYP1, and TYP2 by BJ-5ta-Ex treatment is associated with downregulated MITF expression.

3.3 | BJ-5ta-Ex regulates the cAMP/CREB and ERK signaling pathway

MITF expression is known to be regulated by the cAMP-mediated CREB signaling pathway (Niu & Aisa, 2017). Pretreatment with BJ-5ta-Ex (10^4–10^5 particles/mL) suppressed α-MSH-induced intracellular cAMP levels and phosphorylation of CREB in a dose-dependent manner (Figure 3a,b). BJ-5ta-Ex increased the phosphorylation of extracellular signal-regulated kinase (ERK) (Figure 3c). Furthermore, BJ-5ta-Ex suppressed the α-MSH-induced decrease in p-ERK (extracellular signal-regulated kinase) and increased the protein levels of MITF protein (Figure 3d), indicating that BJ-5ta-Ex induced MITF downregulation by increasing the phosphorylation of ERK at Thr^{202}/Tyr^{204}. To confirm the role of ERK in BJ-5ta-Ex-mediated MITF downregulation, we used PD98059, a potent and selective cell permeable inhibitor of MAP kinase kinase (MEK), to inhibit ERK (Wang et al., 2017). Pretreatment with PD98059 abolished the BJ-5ta-Ex-induced decrease in p-MITF (Ser^{73}) (Figure 3e). At the same time, the downregulation of MITF was blocked, suggesting that the whitening effect of BJ-5ta-Ex was mediated through the activation of the MAPK signaling pathway. Furthermore, through an in situ intracellular tyrosinase activity assay, we confirmed that inhibition of ERK by PD98059 blocked BJ-5ta-Ex-mediated anti-pigmentation (Figure 3f). We confirmed that BJ-5ta-Ex-induced MITF downregulation is mediated by the activation of ERK.

3.4 | BJ-5ta-Ex inhibit the β-catenin signaling pathway

Activation of the β-catenin signaling pathway is known to increase melanin production (Wu & Pan, 2010). Treatment with BJ-5ta-Ex suppressed the α-MSH-induced phosphorylation of AKT (Ser^{473}) and β-catenin and attenuated α-MSH-induced β-catenin expression (Figure 4a,b). Furthermore, we confirmed that inhibition of the β-catenin signaling pathway by BIO, a specific inhibitor of GSK-3β, blocked the anti-melanogenesis effects of BJ-5ta-Ex (Figure 4c). These results suggest that the whitening effect of BJ-5ta-Ex is regulated by the β-catenin signaling pathway.

3.5 | BJ-5ta-Ex inhibited melanosome transport in B16F10 cells

We found that BJ-5ta-Ex treatment reduced the protein levels of rab27a and MLPH but did not influence myosin Va expression (Figure 5a). Furthermore, BJ-5ta-Ex abolished the α-MSH-mediated increase in rab27a and MLPH levels (Figure 5b). We also confirmed that melanosomes were

localized to the perinuclear region and conspicuously absent from the cell periphery in BJ-5ta-Ex-treated B16F10 cells; in contrast, a whole-cell distribution pattern was observed in the control cells (Figure 5c). In mammalian melanocytes, melanosomes are intracellularly transported along microtubules and actin filaments (Kudo et al., 2017). These results suggest that BJ-5ta-Ex also affect melanin transport by downregulating the expression of melanosome transport-related proteins.
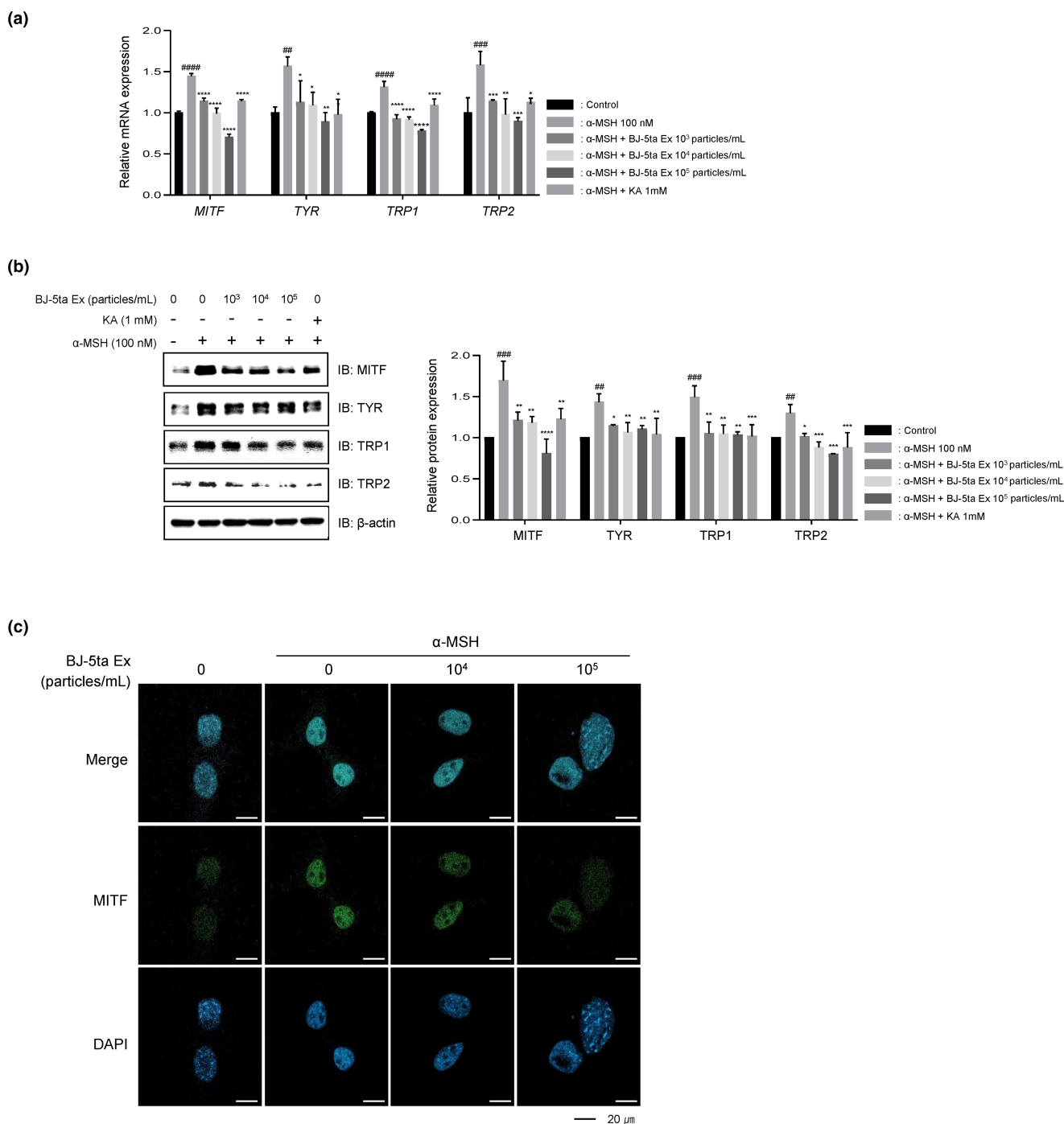

FIGURE 2 Inhibitory effect of BJ-5ta-Ex on melanogenic gene expression. (a, b) The mRNA and protein levels of melanogenesis-related genes including MITF, TYR, TRP1, and TRP2 were determined by RT-qPCR. KA, an established tyrosinase inhibitor, was used as a positive control. (c) MITF (green) and nuclei (blue; counterstained with DAPI). The merged images represent the expression and location of MITF. Scale bar = 20 μm. The results are expressed as the mean ± standard deviation. ##$p < .01$, ###$p < .001$, ####$p < .0001$ compared with the control group (untreated group). *$p < .05$, **$p < .01$, ***$p < .001$, ****$p < .0001$ compared with the α-MSH-treated group.
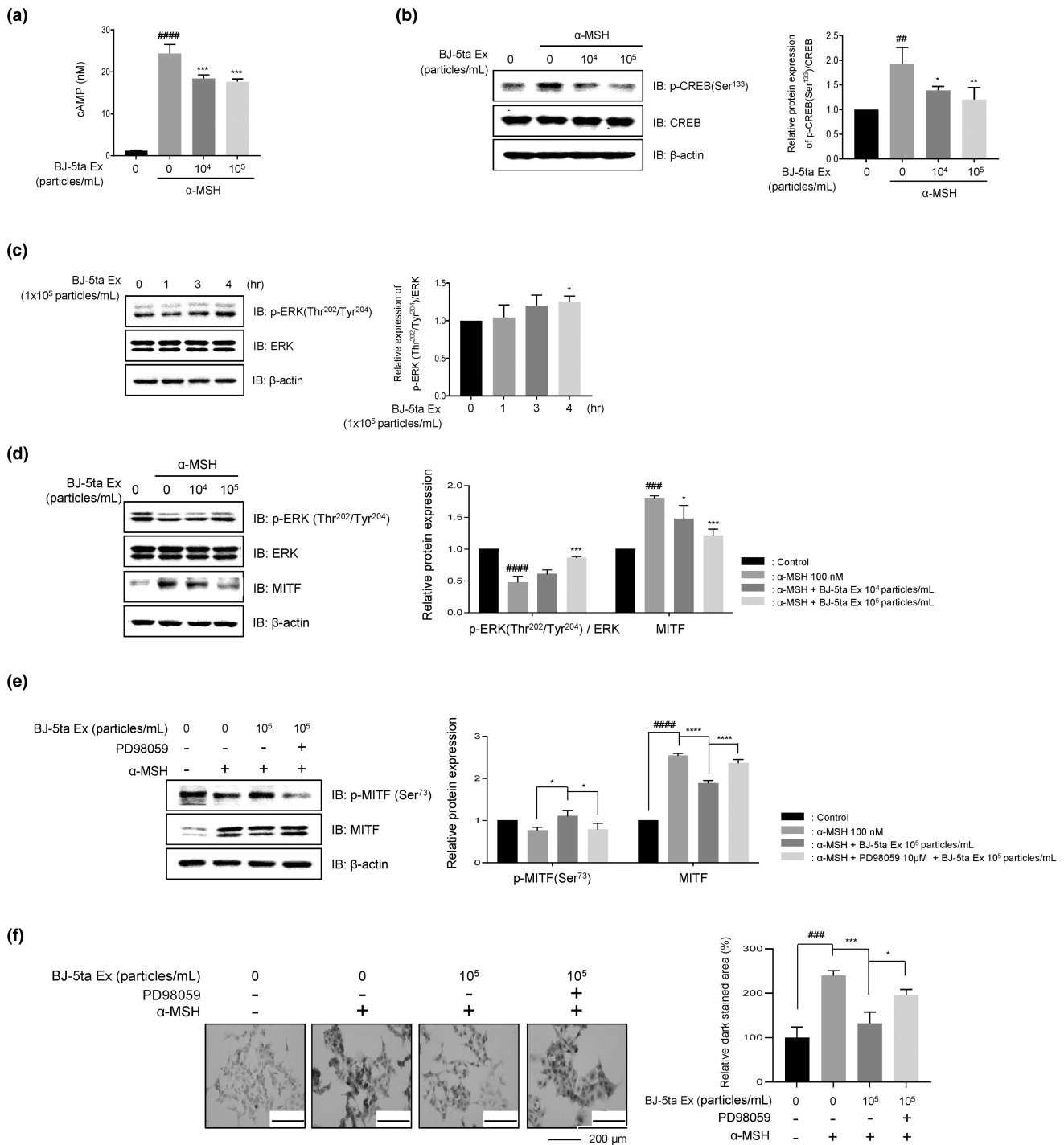
FIGURE 3 BJ-5ta-Ex inhibited melanin production through the cAMP-related pathway and ERK pathway by decreasing MITF expression. (a) Intracellular cAMP levels in B16F10 cells pretreated with BJ-5ta-Ex for 3 h and exposed to α-MSH (100 nM) for 3 min. (b) The protein levels of p-CREB (Ser^{133}) and CREB were assessed by western blotting. (c) Direct effect of BJ-5ta-Ex (10^5 particles/mL) on the protein levels of p-ERK (Thr^{202}/Tyr^{204}) and ERK. (d) Protein expression of p-ERK (Thr^{202}/Tyr^{204}), ERK, and MITF in B16F10 cells pretreated with BJ-5ta-Ex for 3 h and exposed to α-MSH (100 nM) for 1 h. (e, f) Cells were treated with or without α-MSH (100 nM), PD98059 (10 μM), or BJ-5ta-Ex (10^5 particles/mL). Protein expression levels were assessed by western blotting. The in situ intracellular tyrosinase activity was observed via L-DOPA staining. Scale bar = 200 μm. Relative amounts of the stained area were measured with the ImageJ program. The results are expressed as the mean ± standard deviation. ##$p < .01$, ###$p < .001$, ####$p < .0001$ compared with the control group (untreated group). *$p < .05$, **$p < .01$, ***$p < .001$, ****$p < .0001$ compared with the α-MSH-treated group.
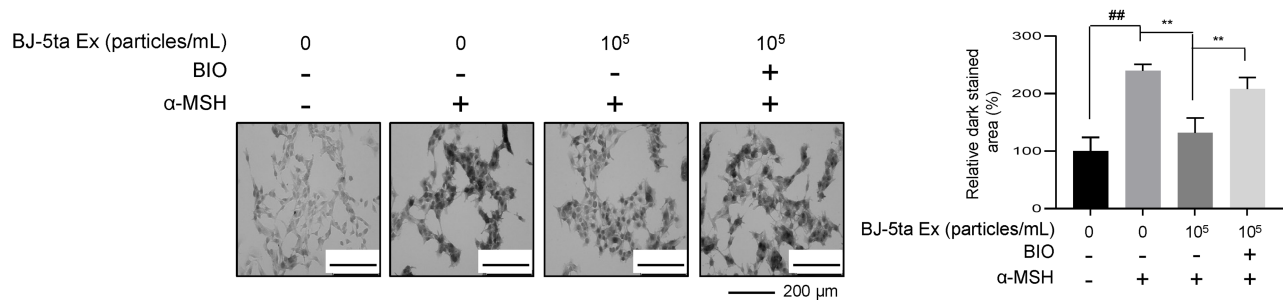
(a)
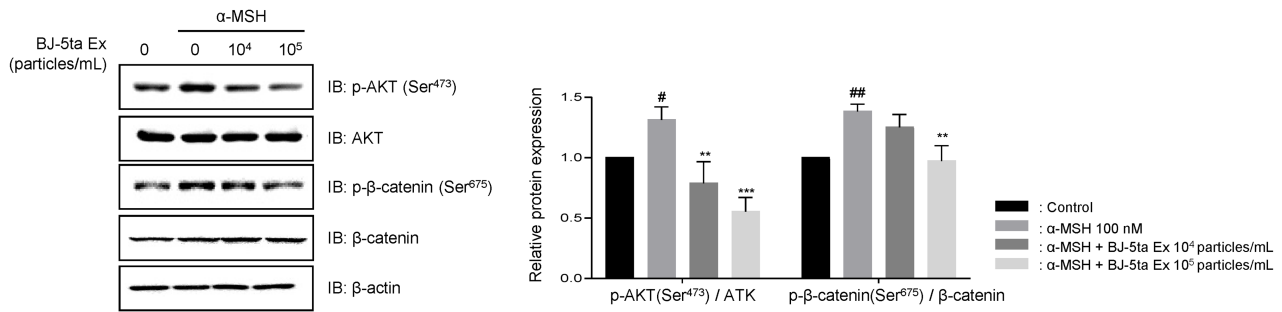
(b)
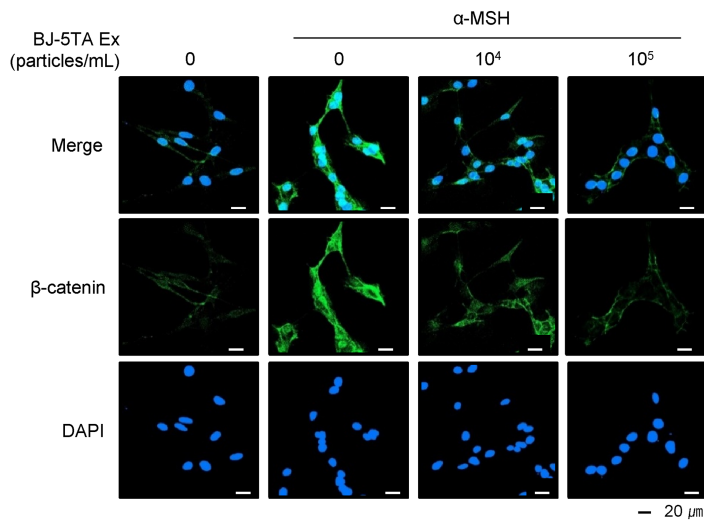
(c)

FIGURE 4 Suppression of the β-catenin signaling pathway in response to treatment with BJ-5ta-Ex. (a) The protein levels of p-Akt (Ser[473]) and Akt were assessed in B16F10 cells pretreated with BJ-5ta-Ex for 3h followed by α-MSH (1nM) treatment for 30min. Expression of p-β-catenin (Ser[675]) and β-catenin in B16F10 cells pretreated with BJ-5ta-Ex for 3h and exposed to α-MSH (100nM) for 1h. (b) β-catenin (green) and nuclei (blue; counterstained with DAPI). The merged images represent the expression and location of β-catenin. Scale bar=20μm. (c) Cells were treated with or without α-MSH (100nM), BIO (1μM), or BJ-5ta-Ex (10[5] particles/mL). The in situ intracellular tyrosinase activity was observed via L-DOPA staining. Scale bar=200μm. Relative amounts of the stained area were measured with the ImageJ program. The results are expressed as the mean±standard deviation. #$p < .05$, ##$p < .01$ compared with the control group (untreated group). **$p < .01$, ***$p < .001$ compared with the α-MSH-treated group.
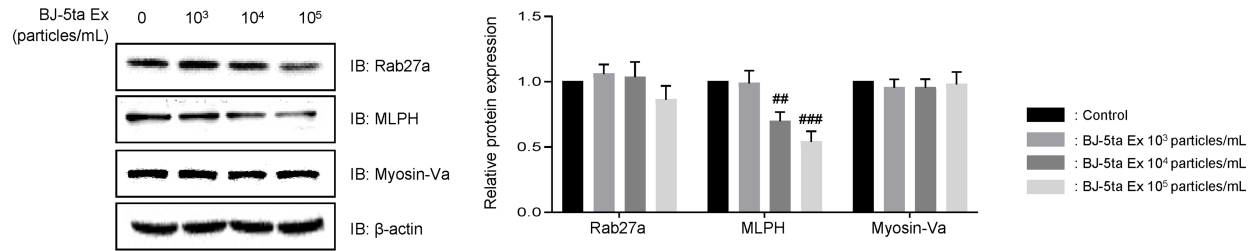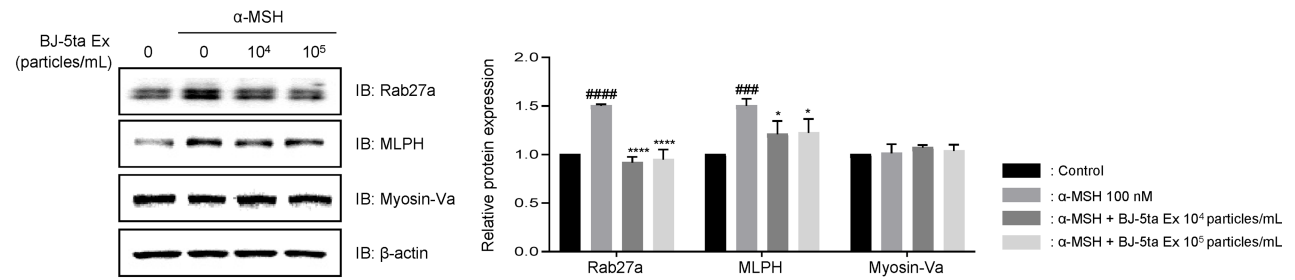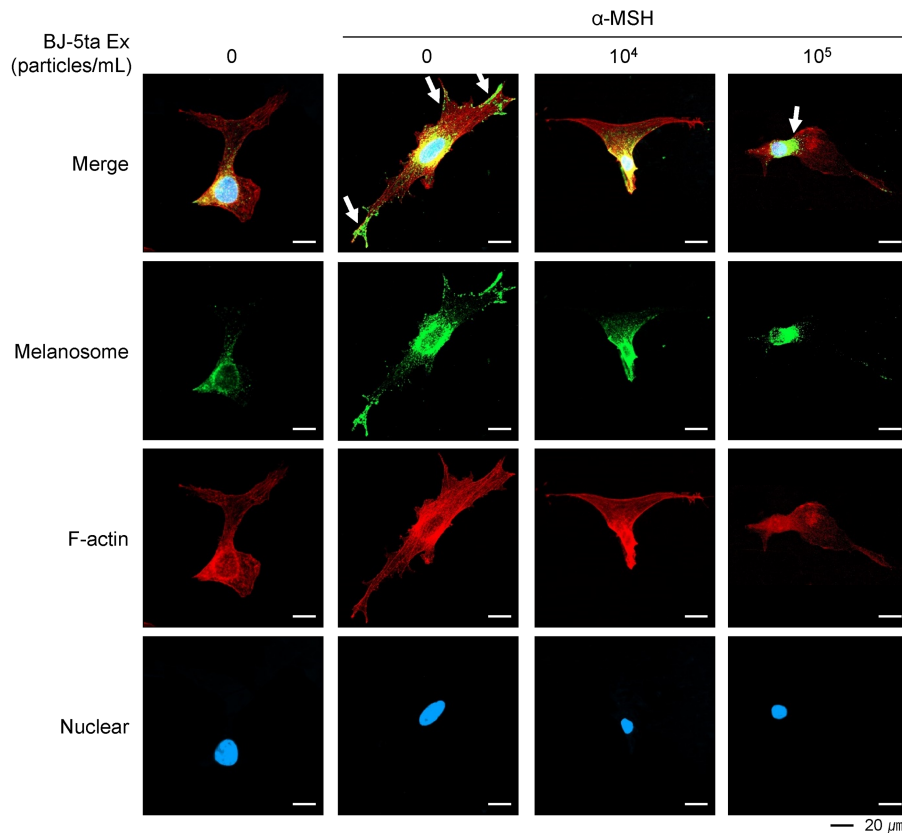
FIGURE 5 Inhibitory effect of BJ-5ta-Ex on melanosome transport. (a) Direct effect of BJ-5ta-Ex on the protein levels of rab27a, MLPH, and myosin Va. (b) Protein levels of rab27a, MLPH, and myosin Va in B16F10 cells pretreated with BJ-5ta-Ex for 3 h and exposed to α-MSH (100 nM) for 24 h. (c) Melanosomes were immunostained with an anti-TRP1 antibody, the nuclei were stained with DAPI, and F-actin was stained with phalloidin. Scale bar = 20 μm. The arrows indicate melanosomes. The results are expressed as the mean ± standard deviation. $\#\#p < .01$, $\#\#\#p < .001$, $\#\#\#\#p < .0001$ compared with the control group (untreated group). $*p < .05$, $****p < .0001$ compared with the α-MSH-treated group.

3.6 | BJ-5ta-Ex alleviated UVB-induced hyperpigmentation in mouse and 3D-RHPE models

First, C57BL/6 mice were subjected to UVB exposure and treated with BJ-5ta-Ex for 3 weeks (Figure 6a). Since mouse ears contain epidermal melanocytes (Gelmi et al., 2022), the efficacy of BJ-5ta-Ex for treating UVB-induced hyperpigmentation was also evaluated on mouse ears. Visible tanning of the ears was observed in the mice treated with UVB, while the UVB-induced alterations in pigmentation were almost completely reversed in the mice treated with BJ-5ta-Ex (Figure 6b). These findings were further confirmed by histological examination. Exposure to UVB induced hyperplasia in the skin, as assessed by H&E staining; however, this effect was reversed by BJ-5ta-Ex treatment (Figure 6c). BJ-5ta-Ex may protect the skin from UVB-induced epidermal thickening. Next, the fluctuations in melanin content were examined by F–M staining and IHC staining for Melan-A. The melanin content and melanin-A expression decreased in a dose-dependent manner in the BJ-5ta-Ex-treated group (Figure 6d,e). TYR expression was also downregulated upon treatment with BJ-5ta-Ex (Figure 6f). Consistent with the anti-pigmentation effects observed in the mouse model, we also confirmed that α-MSH-mediated pigmentation was markedly decreased by treatment with BJ-5ta-Ex in a 3D artificial skin model (Figure 6h). Relative hypopigmentation was also observed using F–M staining (Figure 6i). These results indicate that BJ-5ta-Ex serve as effective inhibitors of hyperpigmentation.

4 | DISCUSSION

Numerous studies have demonstrated the potential of exosomes as novel reagents for use in cell-free therapy because of their high stability, low immunogenicity, and low tumorigenesis (Xiong et al., 2020). Exosomes can be extracted from all types of cells, but most studies published to date have utilized exosomes derived from mesenchymal stem cells (MSCs). However, the isolation of exosomes from MSCs has some disadvantages. First, culture and expansion of MSCs require a significant amount of time, ranging from several days to weeks. Second, during the isolation process, contamination with red blood cells can easily occur. Third, the cell viability is limited. Finally, the isolation of MSCs from bone marrow is an invasive process (Ahmadi & Rezaie, 2021; Horn et al., 2011; Ramakrishnan et al., 2013).

As an alternative, attempts have been made to utilize keratinocyte-derived exosomes, but their effects have been shown to be insignificant compared with those of MSC-derived exosomes. Dermal fibroblasts have recently emerged as an ideal alternative stem cell source for exosome isolation. Dermal fibroblasts, which are located in the dermis of the skin, are essential in skin remodeling, regeneration, and repair. Furthermore, dermal fibroblasts can be isolated from skin using less invasive procedures, are easier to culture, and can be more readily obtained from human foreskin,

which is a type of medical waste, than other cell sources (Han et al., 2021; Oh et al., 2021). Therefore, in the present study, we chose human foreskin fibroblast to evaluate the effect of exosomes on anti-melanogenesis.

Some studies have shown that exosomes from milk and keratinocytes inhibit melanogenesis through exosomal microRNA. For example, exosome-derived microRNA-2478 from milk suppresses melanogenesis through the Akt-GSK3β pathway, and exosomal microRNA-330-5p derived from murine keratinocytes decreases the production of melanin and expression of TYR in melanocytes (Bae & Kim, 2021; Cho et al., 2018; Kim et al., 2014). To date, little research has been done on the effect of exosomes from fibroblasts on whitening.

It is well known that fibroblasts secrete various soluble factors related to melanogenesis. For instance, dickkopf 1 (DKK1) inhibits the β-catenin signaling pathway and decreases the expression of MITF (Yamaguchi et al., 2007). In addition, interleukin-6 (IL-6) exerts an inhibitory effect on TYR activity and melanocyte proliferation, which inhibits melanogenesis (Fu et al., 2020; Swope et al., 1991). On the other hand, keratinocyte growth factor (KGF) (Chen et al., 2010), neuregulin-1(NRG-1) (Choi. et al., 2012), and Hepatocyte growth facor (HGF) are largely described as a mitogenic factor for melatnocytes (Yamamoto et al., 1996) and induce the proliferatoin of melanocytes and melatin production. As evidenced by these findings, fibroblasts contain various soluble factors that can positively or negatively regulate melanogenesis. Therefore, in the present study, we investigated the anti-melanogenic effect of exosomes derived from BJ-5ta human foreskin fibroblasts using B16F10 mouse melanoma cells, mouse model, and dermal reconstitute model.

In general, the majority of depigmenting compounds act specifically to reduce the function of tyrosinase through several mechanisms that include interference with its transcription and/or glycosylation, enzyme inhibition, reduction of byproducts, and post-transcriptional control. As shown in Figure 1e–g, BJ-5ta-Ex inhibit the α-MSH-induced increase in melanin content, intracellular tyrosinase activity, and in situ intracellular tyrosinase activity (Figure 1e–g). However, BJ-5ta-Ex did not show a dose-dependent manner. These results indicated that BJ-5ta-Ex do not control the whitening effect by directly suppressing tyrosinase activity. We further found that BJ-5ta-Ex regulate transcription (MITF mRNA) and phosphorylation (p-MITF at Ser[73]) (Figures 2a and 3e). In addition, the main function of melanin is the protection from photo-damage induced by UVR. However, hyperpigmentation stimulates oxidation reactions and hydrogen peroxide (H_2O_2) generation, which subject melanocytes to oxidative stress (Koga et al., 1992; Simon et al., 2009) and which may cause skin cancer (Sander et al., 2004). Therefore, antioxidant activity in the depigmenting agents is important. Therefore, we evaluated the ROS scavenging activity of BJ-5ta-Ex using the cellular ROS detection assay kit (ab113851, Abcam). As shown in Figure S1. BJ-5ta-Ex treatment significantly decreased the UVB-mediated ROS compared to the control group. These results mean that BJ-5ta-Ex have anti-oxidant activity, which is another factor that regulates the anti-melanogenesis of BJ-5ta-Ex.
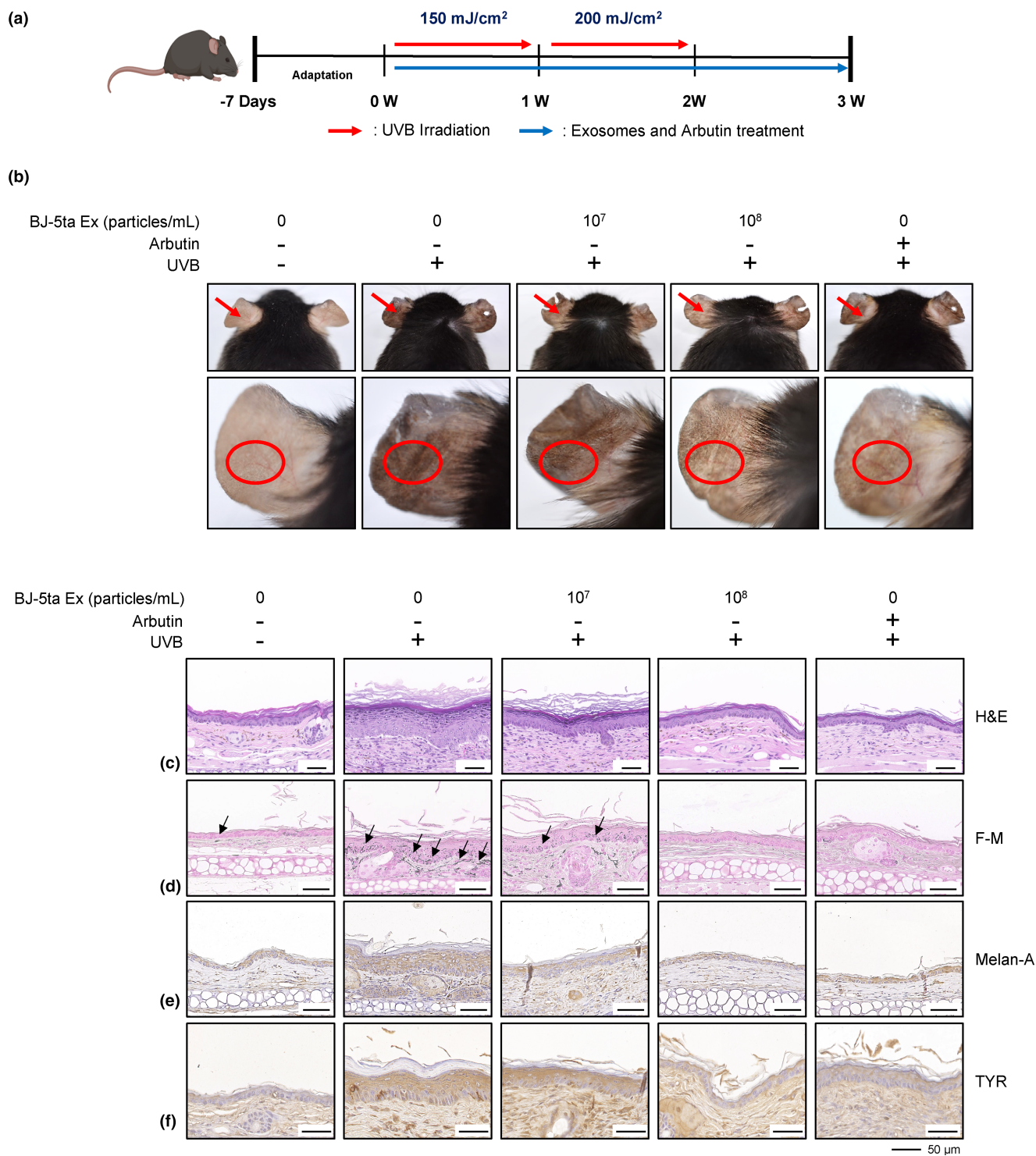
FIGURE 6 Inhibitory effect of BJ-5ta-Ex on melanin production in vivo and a reconstructed human skin model. (a) Schematic diagram of the animal experiments. (b) Photographs demonstrate the skin lightening effect of BJ-5ta-Ex on UVB irradiation-induced hyperpigmentation in C57BL/6 mice following topical application for 3 weeks. (c–f) H&E staining, F–M staining, and histological images of melanin-A and TYR. Scale bar = 50 μm. (g) Schematic diagram of the reconstructed human skin model. (h) Representative images of reconstructed human skin tissue. (i) Melanin pigmentation was observed by F–M staining. Scale bar = 50 μm.

This study has limitations as we only used the mouse melanoma cancer cell line B16F10, which is widely used in many studies on melanin synthesis (Slominski et al., 2004). Therefore, the effect of BJ-5ta-Ex on depigmentation activity in normal human epidermal melanocytes (NHEM) and HMV-II human melanoma cell line will be additionally confirmed in the future. Furthermore, the precise mediators responsible for the effects of BJ-5ta-Ex remain unknown. Therefore, we will perform MALDI-TOF MS profiling to help gain more insights into the composition of BJ-5ta-Ex.
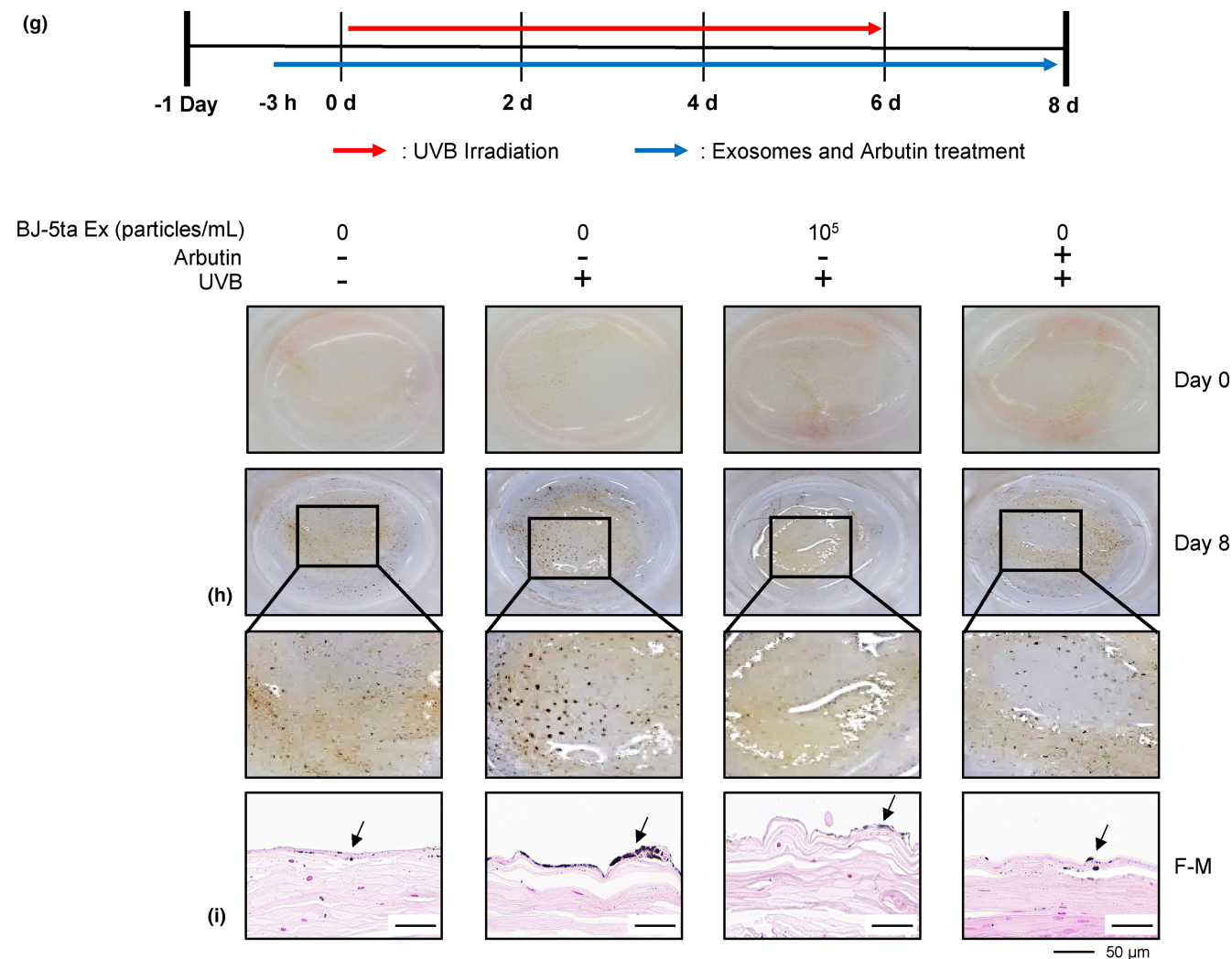
FIGURE 6 (Continued)

In conclusion, these findings reveal the potential role of BJ-5ta-Ex as cosmetic effectors and highlight the significant effects of BJ-5ta-Ex on anti-pigmentation.

AUTHOR CONTRIBUTIONS

Jung Min Lee: Methodology, investigation, data curation, formal analysis, and writing. Jung Ok Lee: Writing, reviewing, and editing. Yujin Kim: Investigation and data curation. You Na Jang: Investigation and data curation. A. Yeon Park: Investigation and data curation. Su-Young Kim: Investigation and data curation. Beom Joon Kim: Reviewing and editing. Kwang-Ho Yoo: Conceptualization, methodology, investigation, and project administration. All authors have read and agreed to the published version of the manuscript.

FUNDING INFORMATION

CONFLICT OF INTEREST STATEMENT

The authors declare that there is no conflict of interest that could be perceived as prejudicing the impartiality of the research reported.

DATA AVAILABILITY STATEMENT

All the data generated and analyzed during this study are included in this article. Further inquiries can be directed to the corresponding author.

ORCID

Jung Min Lee https://orcid.org/0000-0002-4670-2521
Jung Ok Lee https://orcid.org/0000-0002-0048-5322
Yujin Kim https://orcid.org/0000-0002-1247-2887
You Na Jang https://orcid.org/0000-0002-0014-9783
A. Yeon Park https://orcid.org/0000-0002-4667-8875
Su-Young Kim https://orcid.org/0000-0002-3251-5813
Hye Sung Han https://orcid.org/0000-0002-3556-0740
Beom Joon Kim https://orcid.org/0000-0003-2320-7621
Kwang Ho Yoo https://orcid.org/0000-0002-0137-6849

REFERENCES

Ahmadi, M., & Rezaie, J. (2021). Ageing and mesenchymal stem cells derived exosomes: Molecular insight and challenges. *Cell Biochemistry and Function*, 39(1), 60–66. https://doi.org/10.1002/cbf.3602

Bae, I. S., & Kim, S. H. (2021). Milk exosome-derived MicroRNA-2478 suppresses melanogenesis through the Akt-GSK3beta pathway. *Cells*, 10(2848), 1–17. https://doi.org/10.3390/cells10112848

Busca, R., & Ballotti, R. (2000). Cyclic AMP a key messenger in the regulation of skin pigmentation. *Pigment Cell Research*, 13(2), 60–69. https://doi.org/10.1034/j.1600-0749.2000.130203.x

Chang, N. F., Chen, Y. S., Lin, Y. J., Tai, T. H., Chen, A. N., Huang, C. H., & Lin, C. C. (2017). Study of hydroquinone mediated cytotoxicity and hypopigmentation effects from UVB-irradiated arbutin and DeoxyArbutin. *International Journal of Molecular Sciences*, 18(5), 969. https://doi.org/10.3390/ijms18050969

Chen, N., Hu, Y., Li, W. H., Eisinger, M., Seiberg, M., & Lin, C. B. (2010). The role of keratinocyte growth factor in melanogenesis: A possible mechanism for the initiation of solar lentigines. *Experimental Dermatology*, 19(10), 865–872. https://doi.org/10.1111/j.1600-0625.2009.00957.x

Cho, B. S., Kim, J. O., Ha, D. H., & Yi, Y. W. (2018). Exosomes derived from human adipose tissue-derived mesenchymal stem cells alleviate atopic dermatitis. *Stem Cell Research & Therapy*, 9(1), 187. https://doi.org/10.1186/s13287-018-0939-5

Choi, W., Kolbe, L., & Hearing, V. J. (2012). Characterization of the bioactive motif of neuregulin-1, a fibroblast-derived paracrine factor that regulates the constitutive color and the function of melanocytes in human skin. *Pigment Cell & Melanoma Research*, 25(4), 477–481. https://doi.org/10.1111/j.1755-148X.2012.01002.x

Clarys, P., Alewaeters, K., Lambrecht, R., & Barel, A. O. (2000). Skin color measurements: comparison between three instruments: The Chromameter(R), the DermaSpectrometer(R) and the Mexameter(R). *Skin Research and Technology*, 6(4), 230–238. https://doi.org/10.1034/j.1600-0846.2000.006004230.x

Desmedt, B., Ates, G., Courselle, P., De Beer, J. O., Rogiers, V., Hendrickx, B., Deconinck, E., & De Paepe, K. (2016). In vitro dermal absorption of hydroquinone: Protocol validation and applicability on illegal skin-whitening cosmetics. *Skin Pharmacology and Physiology*, 29(6), 300–308. https://doi.org/10.1159/000454719

Fu, C., Chen, J., Lu, J., Yi, L., Tong, X., Kang, L., Pei, S., Ouyang, Y., Jiang, L., Ding, Y., Zhao, X., Li, S., Yang, Y., Huang, J., & Zeng, Q. (2020). Roles of inflammation factors in melanogenesis (review). *Molecular Medicine Reports*, 21(3), 1421–1430. https://doi.org/10.3892/mmr.2020.10950

Fukuda, M. (2021). Rab GTPases: Key players in melanosome biogenesis, transport, and transfer. *Pigment Cell & Melanoma Research*, 34(2), 222–235. https://doi.org/10.1111/pcmr.12931

Gaur, M., Dobke, M., & Lunyak, V. V. (2017). Mesenchymal stem cells from adipose tissue in clinical applications for dermatological indications and skin aging. *International Journal of Molecular Sciences*, 18(1), 208. https://doi.org/10.3390/ijms18010208

Gelmi, M. C., Houtzagers, L. E., Strub, T., Krossa, I., & Jager, M. J. (2022). MITF in normal melanocytes, cutaneous and uveal melanoma: A delicate balance. *International Journal of Molecular Sciences*, 23(11), 6001. https://doi.org/10.3390/ijms23116001

Han, X., Wu, P., Li, L., Sahal, H. M., Ji, C., Zhang, J., Wang, Y., Wang, Q., Qian, H., Shi, H., & Xu, W. (2021). Exosomes derived from autologous dermal fibroblasts promote diabetic cutaneous wound healing through the Akt/beta-catenin pathway. *Cell Cycle*, 20(5–6), 616–629. https://doi.org/10.1080/15384101.2021.1894813

Hearing, V. J. (2011). Determination of melanin synthetic pathways. *The Journal of Investigative Dermatology*, 131(E1), E8–E11. https://doi.org/10.1038/skinbio.2011.4

Hong, P., Yang, H., Wu, Y., Li, K., & Tang, Z. (2019). The functions and clinical application potential of exosomes derived from adipose mesenchymal stem cells: A comprehensive review. *Stem Cell Research & Therapy*, 10(1), 242. https://doi.org/10.1186/s13287-019-1358-y

Horn, P., Bork, S., & Wagner, W. (2011). Standardized isolation of human mesenchymal stromal cells with red blood cell lysis. *Methods in Molecular Biology*, 698, 23–35. https://doi.org/10.1007/978-1-60761-999-4_3

Hsiao, J. J., & Fisher, D. E. (2014). The roles of microphthalmia-associated transcription factor and pigmentation in melanoma. *Archives of Biochemistry and Biophysics*, 563, 28–34. https://doi.org/10.1016/j.abb.2014.07.019

Hume, A. N., Tarafder, A. K., Ramalho, J. S., Sviderskaya, E. V., & Seabra, M. C. (2006). A coiled-coil domain of melanophilin is essential for myosin Va recruitment and melanosome transport in melanocytes. *Molecular Biology of the Cell*, 17(11), 4720–4735. https://doi.org/10.1091/mbc.e06-05-0457

Hume, A. N., Ushakov, D. S., Tarafder, A. K., Ferenczi, M. A., & Seabra, M. C. (2007). Rab27a and MyoVa are the primary Mlph interactors regulating melanosome transport in melanocytes. *Journal of Cell Science*, 120(Pt 17), 3111–3122. https://doi.org/10.1242/jcs.010207

Jiang, M., Fang, H., Shao, S., Dang, E., Zhang, J., Qiao, P., Yang, A., & Wang, G. (2019). Keratinocyte exosomes activate neutrophils and enhance skin inflammation in psoriasis. *The FASEB Journal*, 33(12), 13241–13253. https://doi.org/10.1096/fj.201900642R

Kim, E. S., Park, S. J., Goh, M. J., Na, Y. J., Jo, D. S., Jo, Y. K., Shin, J. H., Choi, E. S., Lee, H. K., Kim, J. Y., Jeon, H. B., Kim, J. C., & Cho, D. H. (2014). Mitochondrial dynamics regulate melanogenesis through proteasomal degradation of MITF via ROS-ERK activation. *Pigment Cell & Melanoma Research*, 27(6), 1051–1062. https://doi.org/10.1111/pcmr.12298

Koga, S., Nakano, M., & Tero-Kubota, S. (1992). Generation of superoxide during the enzymatic action of tyrosinase. *Archives of Biochemistry and Biophysics*, 292(2), 570–575. https://doi.org/10.1016/0003-9861(92)90032-r

Kudo, M., Kobayashi-Nakamura, K., & Tsuji-Naito, K. (2017). Bifunctional effects of O-methylated flavones from Scutellaria baicalensis Georgi on melanocytes: Inhibition of melanin production and intracellular melanosome transport. *PLoS One*, 12(2), e0171513. https://doi.org/10.1371/journal.pone.0171513

Li, M., Wang, T., Tian, H., Wei, G., Zhao, L., & Shi, Y. (2019). Macrophage-derived exosomes accelerate wound healing through their anti-inflammation effects in a diabetic rat model. *Artificial Cells, Nanomedicine, and Biotechnology*, 47(1), 3793–3803. https://doi.org/10.1080/21691401.2019.1669617

Nakagawa, M., Kawai, K., & Kawai, K. (1995). Contact allergy to kojic acid in skin care products. *Contact Dermatitis*, 32(1), 9–13. https://doi.org/10.1111/j.1600-0536.1995.tb00832.x

Niu, C., & Aisa, H. A. (2017). Upregulation of melanogenesis and tyrosinase activity: Potential agents for vitiligo. *Molecules*, 22(8), 1303. https://doi.org/10.3390/molecules22081303

Oh, E. J., Gangadaran, P., Rajendran, R. L., Kim, H. M., Oh, J. M., Choi, K. Y., Chung, H. Y., & Ahn, B. C. (2021). Extracellular vesicles derived from fibroblasts promote wound healing by optimizing fibroblast and endothelial cellular functions. *Stem Cells*, 39(3), 266–279. https://doi.org/10.1002/stem.3310

Ramakrishnan, A., Torok-Storb, B., & Pillai, M. M. (2013). Primary marrow-derived stromal cells: Isolation and manipulation. *Methods in Molecular Biology*, 1035, 75–101. https://doi.org/10.1007/978-1-62703-508-8_8

Sander, C. S., Chang, H., Hamm, F., Elsner, P., & Thiele, J. J. (2004). Role of oxidative stress and the antioxidant network in cutaneous carcinogenesis. *International Journal of Dermatology*, 43(5), 326–335. https://doi.org/10.1111/j.1365-4632.2004.02222.x

Shoag, J., Haq, R., Zhang, M., Liu, L., Rowe, G. C., Jiang, A., Koulisis, N., Farrel, C., Amos, C. I., Wei, Q., Lee, J. E., Zhang, J., Kupper, T. S., Qureshi, A. A., Cui, R., Han, J., Fisher, D. E., & Arany, Z. (2013). PGC-1 coactivators regulate MITF and the tanning response. *Molecular Cell*, *49*(1), 145–157. https://doi.org/10.1016/j.molcel.2012.10.027

Simon, J. D., Peles, D., Wakamatsu, K., & Ito, S. (2009). Current challenges in understanding melanogenesis: Bridging chemistry, biological control, morphology, and function. *Pigment Cell & Melanoma Research*, *22*(5), 563–579. https://doi.org/10.1111/j.1755-148X.2009.00610.x

Slominski, A., Tobin, D. J., Shibahara, S., & Wortsman, J. (2004). Melanin pigmentation in mammalian skin and its hormonal regulation. *Physiological Reviews*, *84*(4), 1155–1228. https://doi.org/10.1152/physrev.00044.2003

Speeckaert, R., Van Gele, M., Speeckaert, M. M., Lambert, J., & van Geel, N. (2014). The biology of hyperpigmentation syndromes. *Pigment Cell & Melanoma Research*, *27*(4), 512–524. https://doi.org/10.1111/pcmr.12235

Swope, V. B., Abdel-Malek, Z., Kassem, L. M., & Nordlund, J. J. (1991). Interleukins 1 alpha and 6 and tumor necrosis factor-alpha are paracrine inhibitors of human melanocyte proliferation and melanogenesis. *The Journal of Investigative Dermatology*, *96*(2), 180–185. https://doi.org/10.1111/1523-1747.ep12460991

Wang, K., Hou, Y., Gu, C., Zhao, D., Duan, Y., Ran, Z., Li, Q., & Li, X. (2017). Inhibitory effect of the mitogen activated protein kinase specific inhibitor PD98059 on Mtb-Ag-activated gammadeltaTau cells. *International Journal of Clinical and Experimental Pathology*, *10*(9), 9644–9648.

Wu, D., & Pan, W. (2010). GSK3: A multifaceted kinase in Wnt signaling. *Trends in Biochemical Sciences*, *35*(3), 161–168. https://doi.org/10.1016/j.tibs.2009.10.002

Wu, X., Sakamoto, T., Zhang, F., Sellers, J. R., & Hammer, J. A., 3rd. (2006). In vitro reconstitution of a transport complex containing Rab27a, melanophilin and myosin Va. *FEBS Letters*, *580*(25), 5863–5868. https://doi.org/10.1016/j.febslet.2006.09.047

Xiong, J., Liu, Z., Wu, M., Sun, M., Xia, Y., & Wang, Y. (2020). Comparison of proangiogenic effects of adipose-derived stem cells and foreskin fibroblast exosomes on artificial dermis prefabricated flaps. *Stem Cells International*, *2020*, 5293850. https://doi.org/10.1155/2020/5293850

Yamaguchi, Y., Passeron, T., Watabe, H., Yasumoto, K., Rouzaud, F., Hoashi, T., & Hearing, V. J. (2007). The effects of dickkopf 1 on gene expression and Wnt signaling by melanocytes: Mechanisms underlying its suppression of melanocyte function and proliferation. *The Journal of Investigative Dermatology*, *127*(5), 1217–1225. https://doi.org/10.1038/sj.jid.5700629

Yamamoto, T., Katayama, I., & Nishioka, K. (1996). Impaired expression of stem cell factor in dermatofibroma fibroblasts. *Acta Dermato-Venereologica*, *76*(4), 257–259. https://doi.org/10.2340/0001555576257259

Zhang, Y., Liu, Y., Liu, H., & Tang, W. H. (2019). Exosomes: Biogenesis, biologic function and clinical potential. *Cell & Bioscience*, *9*, 19. https://doi.org/10.1186/s13578-019-0282-2

Zilles, J. C., Dos Santos, F. L., Kulkamp-Guerreiro, I. C., & Contri, R. V. (2022). Biological activities and safety data of kojic acid and its derivatives: A review. *Experimental Dermatology*, *31*(10), 1500–1521. https://doi.org/10.1111/exd.14662

SUPPORTING INFORMATION

Additional supporting information can be found online in the Supporting Information section at the end of this article.